06

Effect of synthesis conditions on the structure and optical properties of a-C:H films

© A.P. Ryaguzov,[1] A.R. Assembayeva,[1,2] F. Bekmurat,[1,3] R.R. Nemkayeva,[1] M.F. Kadir[1]

[1] National Open-Type Nanotechnology Laboratory al-Farabi Kazakh National University,
050040 Almaty, Kazakhstan
[2] Satbayev University,
050040 Almaty, Kazakhstan
[3] Department of Solid State Physics and Nonlinear Physics, al-Farabi Kazakh National University,
050040 Almaty, Kazakhstan
e-mail: a.assembayeva@satbayev.university

Received November 22, 2024
Revised November 22, 2024
Accepted November 22, 2024

The results of the study on amorphous hydrogenated carbon (a-C:H) films obtained by magnetron sputtering are presented. The influence of ion-plasma discharge power on the formation of the local structure of a-C:H films was investigated using Raman scattering spectroscopy. The paper demonstrates how the synthesis conditions affect the sp^2/sp^3- bond ratio in the formation of the a-C:H film structure and, as a result, the change in their optical properties. The optical band gap values for a-C:H films synthesized at different discharge power levels were calculated. It was found that increasing the ion-plasma discharge power from 12 to 18 W leads to a decrease in the optical band gap from 1.8 to 1.43 eV.

Keywords: amorphous hydrogenated diamond-like carbon films, magnetron sputtering, raman spectroscopy, optical band gap.

DOI: 10.61011/TP.2025.02.60841.420-24

Introduction

Production of nanostructured carbon-based materials has become one of the key nanotechnology areas in recent years. Carbon ability to form various electronic configurations makes it possible to synthesize nanomaterials with a wide range of unique properties. Depending on the ratio of thesp^3- and sp^2-hybridized carbon bonds, crystalline solid bodies, disordered structures and polymer-like materials may be produced.

Among low-dimensional carbon structures, amorphous carbon films (a-C) that contain carbon atoms in hybridization states of the sp^3-, sp^2- and sp^1-bonds, and structures consisting of sp^2- and sp^1-sites passivated by hydrogen (H) atoms are of special interest. According to A.C. Ferrari's and J. Robertson's ternary diagram [1] that characterizes „carbon-hydrogen" compounds, the key parameters for amorphous carbon classification are the ratio of sp^2/sp^3-bonded sites and hydrogen content that further define the physical and chemical properties of a-C and a-C:H. The content of sp^2- and sp^3-bonded sites in the amorphous carbon structure may vary from ~ 10 to ~ 90 at.% depending on the synthesis conditions. Depending on the number of sp^2- and sp^3-sites, the structure varies in a wide range — from graphite-like to diamond-like. Moreover, hydrogen concentration and formation of C−H-bonds considerably affect the structure formation and can change the structure from diamond-like to polymer-like.

Amorphous carbon with the content of sp^3-sites more than 40% is called diamond-like carbon (ta-C or DLC) and has properties that are close to diamond properties [1]. The diamond-like shape of carbon includes both thesp^3 bonds and sp^2-σ bonds, and forms a tetrahedral structure from the sp^3-sites. A carbon atom in the sp^2-hybridization has a π-electron that is not bound to the structure and affects the electronic properties of the material. Introduction of H atoms into the amorphous diamond-like carbon film structure during synthesis may change the structural characteristics significantly and affect the ratio of sp^2- and sp^3-sites. H atoms passivate theπ-electrons of sp^2-hybridized bonds leading to a change in the number of sp^3-sites and, thus, to a change in mechanical and electrical properties of the material.

Thin-film coatings are formed on the basis of hydrogenated amorphous carbon (a-C:H) and find wide application in various industries due to their exclusive properties such as low friction coefficient, high hardness, durability, chemical inertness, optical transparency and biocompatibility [2,3]. These properties are attributable to a complex configuration of amorphous matrix consisting of C−C- and C−H-bonds. Unique properties of a-C:H-films and their parametric tunability in wide ranges are of high interest to developers of new instruments and devices facilitating the use of structures based on the hydrogenated diamond-like carbon films as passive and active elements of electronic and optical equipment.

Physical and chemical properties of hydrogenated amorphous films are susceptible to significant changes depending on the synthesis technique and conditions. Various approaches to fabricating nanoscale a-C:H-films have been currently developed, including chemical vapor deposition [4], pulsed laser deposition [5] and cathodic arc deposition [6].

Chemical vapor deposition (CVD) and physical vapor deposition (PVD) are the most widely used hydrogenated amorphous carbon films synthesis processes. The CVD process is used to deposit highly homogeneous a-C:H-coatings onto large surfaces. a-C:H films produced using CVD from hydrocarbon precursors may take shapes from hydrogenated carbon to hydrated tetrahedral carbon (ta-C:H), that differ in the number of sites in the sp^3-hybridized state and H content. However, deposition of a-C:H-films using the CVD method is generally based on the utilization of volatile precursors which limits and complicates the metallic impurity deposition process during synthesis.

This study uses a magnetron ion-plasma sputtering method that provides films with various structures and properties by varying the plasma-supporting gas composition and synthesis process variables. Possibility to modify carbon films in a wide range of thermodynamic conditions is the advantage of this method. Importance of adherence to particular process parameters for producing a-C-films with high contents of Cp^3-hybridized bonds has been already discussed before in [7]. Moreover, the advantages of the process include impurity modification using nanoparticles of various metals. Varying the synthesis conditions for structural modification offers the opportunities for targeted influence on the formation of a-C:H-film structure and properties.

1. Experimental procedure

Amorphous a-C:H carbon films were synthesized using the magnetron ion-plasma sputtering process in argon-hydrogen plasma. A carbon plate with purity 99.9999 at.%, argon gas (99.9999 at.%) and hydrogen gas (99.9999 at.%) were used as feedstock. A polycrystalline carbon target is made by Zhongnuo Xin (Beijing) Technology Co. Ltd. (China). The carbon target underwent additional treatment in hydrochloric acid. Argon gas was filtered in the Epishur unit (Russia). High purity hydrogen was obtained using the GBCh-16M1 (Russia) hydrogen generator. Films were synthesized on KU-1 (equivalent to JGS1) quartz and crystalline silicon (100) wafers with a resistivity of $\sim 0.01\,\Omega\cdot$cm. Silicon (100) and quartz wafers were purchased from Changchun Yutai Optics Co. Ltd. (China). Energy of atom and molecule condensation on substrate and the sputtering process were defined by the plasma discharge power. Synthesis of nanostructured carbon films was performed in DC plasma and at plasma discharge power (P) of 12 W, 15 W and 18 W. Argon gas (Ar) and hydrogen gas (H_2) flow rates for the synthesis were 25 Sccm and 4 Sccm, respectively. The substrate temperature was controlled using a copper-constantan thermocouple. Substrate temperature was 323 K max. Film thickness was measured on a fresh cleavage face of a silicon wafer using the Quanta 200i 3D scanning-electron microscope (FEI, USA). Thickness measurement is illustrated in Figure 1.

a-C:H diamond-like thin films were synthesized on the TSU-600 magnetron sputtering system (Beijing Technology Science Co., Ltd., China) equipped with the sputtering process variable monitoring system, vacuum pumping system and water cooling. The pumping system consisted of volute and turbomolecular pumps. Residual gases in the process chamber volume were controlled by the mass-spectrometry method using the Extorr XT-100 series residual gas analyzer. Residual gas analyses using the Extorr XT-100 mass-spectrometer showed that water vapor pressure after pumping during 30 min was equal to $\sim 10^{-8}$ Torr. Partial oxygen and nitrogen pressure was $\sim 10^{-9}$ Torr, while the pressure of other gases varied within 10^{-10} and 10^{-11} Torr. The process physics and synthesis technique are described in more detail in [7].

Atomic-force microscopy (AFM) method was used to examine the features of the synthesized diamond-like sample structure and surface morphology using the Solver Spectrum system (NT-MTD, Russia).

The effect of ion-plasma discharge power on the local structure formation of the synthesized diamond-like films was examined by the Raman scattering (RS) method that is widely used to study carbon material structure. The experiments were carried out on the NTegra Spectra system (NT-MTD, Russia).

The ellipsometry method was used to measure the refractive index of (n) a-C:H-films synthesized on quartz substrates. Measurements were performed using the Horiba Uvisel Plus ellipsometer at a photon energy from 0.5 eV to 7 eV and incident angle 55°58′. Ellipsometric data

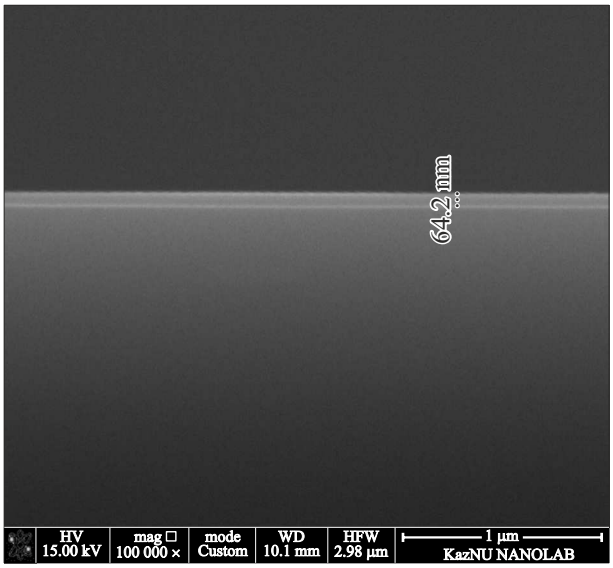

Figure 1. Determining a-C:H-film thickness on the scanning-electron microscope.

was analyzed using DeltaPsi2 integrated software package that controls the entire family of HORIBA Scientific spectroscopic ellipsometers and reflectometers. Optical band gap (E_g) was evaluated by the transmission and reflection spectra measured using the Lambda 35 spectrophotometer (Perkin Elmer, USA). Data obtained by the spectrophotometer method was used to evaluate the effect of synthesis conditions on the optical properties of hydrogenated carbon films.

2. Findings and discussion

2.1. AFM examination of the a-C:H-film surface morphology

Synthesized sample surface morphology was studied by the AFM method in semi-contact mode. For each of the samples, AFM images of surface with the scanning area of $3 \times 3\,\mu$m were made. The NSG01 probes with a radius of rounding of 10 nm and vibration frequency of $\sim 150 \pm 50$ kHz were used for the measurement.

Figure 2 shows the changes in surface morphology of the hydrogenated a-C:H samples synthesized at 12 W, 15 W and 18 W. For more detailed study of the DC discharge power effect on the surface morphology variation on the AFM images, the surface roughness of a-C:H films was evaluated by choosing a random scanning direction along the X axis. Figure 2, a, shows that a sample made at $P = 12$ W has a porous surface with globules whose maximum size at the base is approx. 80 nm with height differences along the Z axis of about 0.75 nm; the distance between them varies from 100 nm to 200 nm. Morphology of the synthesized samples is defined by nanoscale textural features in the form of pores and peaks. Some features may be associated with local changes in the film surface structure consisting of the sp^2-clusters embedded in the sp^3-site matrix. Scanning of samples made at higher discharge powers showed that no significant changes in sizes along the X axis were observed (Figure 2, *d, f*), nevertheless, when P increases, height difference variations are observed along the Z axis. Increase in the power leads to a decease in nanoscale structures described above, therefore large formations in the form of globules with the maximum height 3.5 nm and base dimension 60 nm are observed. Other pores and globules with different sizes are also present and shown in Figure 2, *d*. Further increase in the discharge power as shown in Figure 2, *f* leads to a decrease in the globule and pore sizes, which is probably due to higher activation of atoms and molecules that have higher energy. Such behavior results in the uniform atom distribution on the surface.

From the AFM surface morphology analysis it follows that the surface roughness of a-C:H films increases with the ion-plasma discharge power growth. Formation of film surface morphology depends significantly on the atom and molecule condensation energy. Change in the synthesis conditions causes condensation condition variations due to the change in atom, molecule and ion energy and density.

At low discharge powers, the energy of argon ions that bomb the target is low which causes a low energy of condensed substance. This hinders formation of larger structures. Increase in the discharge energy causes the increase in condensed particle diffusion, which in turn facilitates the increase in surface migration. As a result, „bombardment“ of high-energy carbon atoms takes place in the film surface area, which affects the surface formation process significantly. Thus, it is likely that the degree of surface migration and diffusion of condensed atoms increases as the discharge power grows, thus, changing the surface morphology of synthesized films.

2.2. RS examination of the local structure of a-C:H films depending on the DC discharge power

The affect of synthesis parameters on the structure formation was identified by the RS method that is used to determine the differences in the local structure of amorphous carbon films depending on the synthesis conditions. The local structure of synthesized a-C:H films features the presence of the sp^3 and sp^2 bonds. Additional parameters obtained from the RS analysis such as base peak positions and FWHM, and intensity ratios of D, T and G peaks (I_D/I_G and I_T/I_G) are used for indirect evaluation of sp^2/sp^3-hybridized bonds in the amorphous carbon film structures. Introduction of H atoms into the a-C-film structure leads to passivation of unbound π-electrons and formation of additional C−H-bonds, thus, facilitating the increase in sp^3-hybridized carbon atoms. Consequently, correlation between the content of sp^3-bound sites and RS characteristics may differ considerably for a-C:H with different H content. For the purpose of this work, the content of sp^3-sites means the total number of C−C and C−H sp^3- hybridized bonds.

Figure 3 shows the RS spectra of a-C:H films synthesized on silicon and quartz plates using the 473 nm excitation laser. Raman scattering examination of the a-C:H film structure has shown the presence of bands typical of amorphous carbon structures. These films are characterized by the base G peak in the $1500-1600\,\text{cm}^{-1}$ frequency region, a shoulder in the low-frequency region from 1000 to $1400\,\text{cm}^{-1}$ and second-order band in the $3000\,\text{cm}^{-1}$ region [8] (Figure 3). The first sharp peak at $519\,\text{cm}^{-1}$ in the spectra of samples synthesized on Si substrates (Figure 3, *b*) and the second-order phonon band in the $980\,\text{cm}^{-1}$ region correspond to the silicon substrate phonon spectrum.

Moreover, it may be noted that the RS spectra of all a-C:H samples synthesized both on silicon and quartz substrates demonstrate a high-frequency spectrum slope. This RS spectrum slope is associated with photoluminescence (PL) caused by unbound π-electrons in the sp^2-sites [9]. According to Robertson's cluster model [10], the hydrogenated carbon film structure consists of the sp^2-hybridized carbon bond clusters

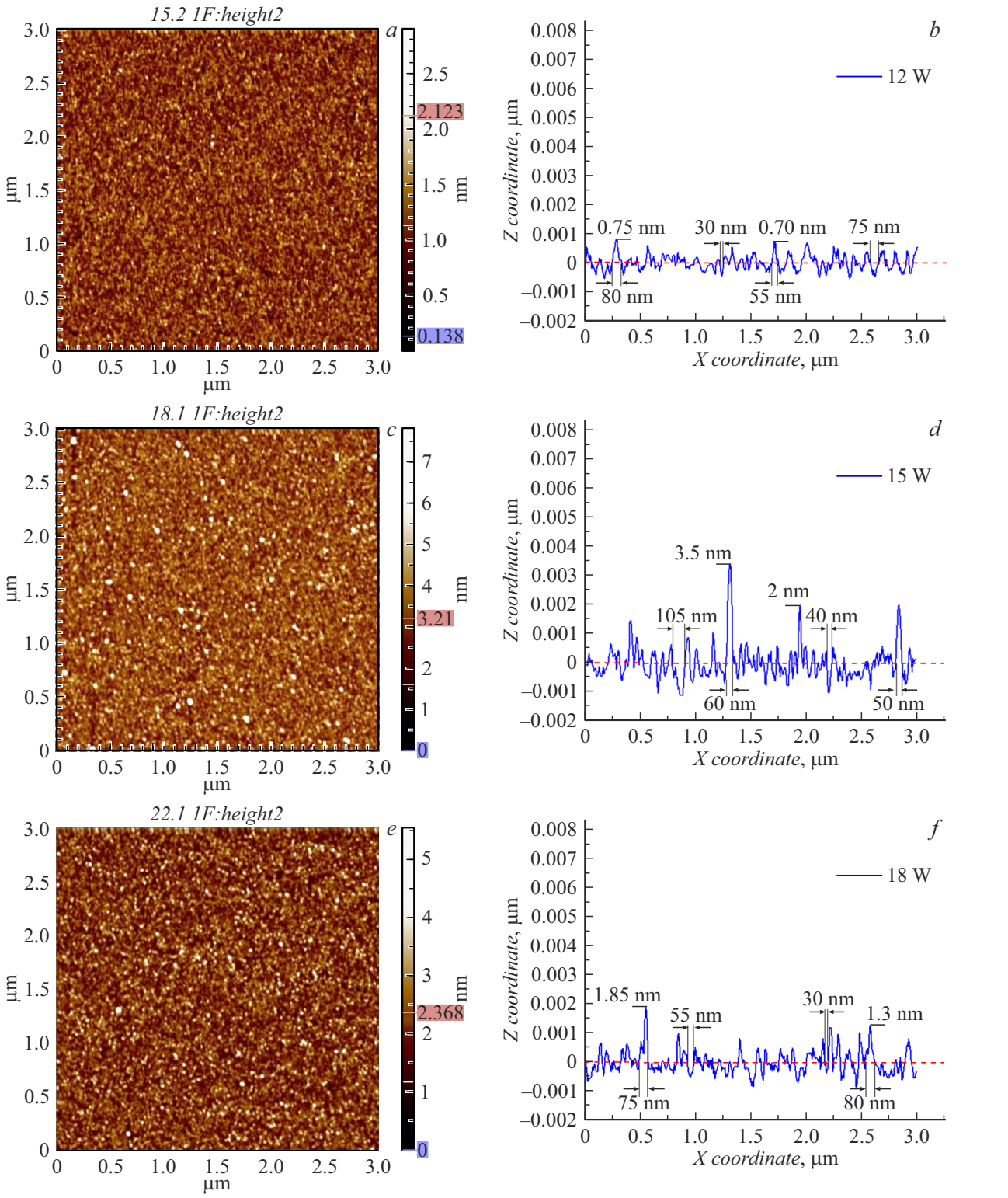

Figure 2. Morphology of a-C:H-films synthesized at P, $W = 12$ (a, b), 15 (c, d), 18 (e, f).

in the sp^3-site matrix. PL in such films is caused by the recombination of electron-hole pairs of the sp^2-sites.

As can be seen from Figure 3, the most pronounced PL slope is observed for films synthesized at low discharge powers. PL reduction is associated with the reduced number of sp^2-sites per unit volume. Thus, the change of plasma discharge power gives rise to the change of structure formation or sp^2/sp^3-sites, which in turn influences the PL level.

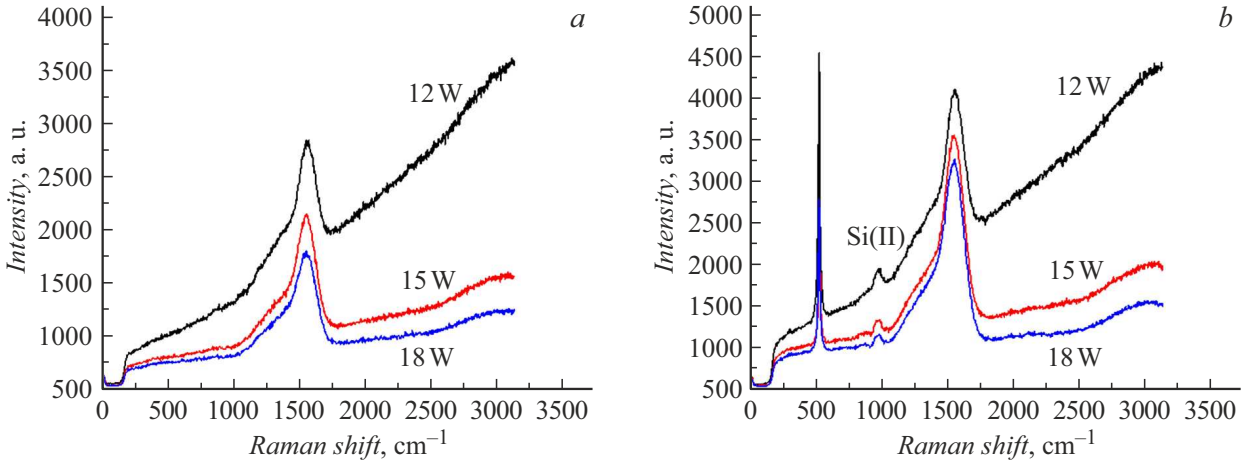

Figure 3. RS spectra of a-C:H-films synthesized on quartz (a) and silicon (100) substrates (b) in different synthesis conditions.

For more detailed analysis of the plasma power influence on the formation of local a-C:H film structure, the RS spectra were decomposed according to the normal distribution into components characterizing the density of phonon states. Decomposition was performed into the minimum number of peaks whose resultant accurately described the experimental curve. Reliability of decomposition or coincidence of the experimental curve with the decomposition resultant was $R^2 > 0.99$. Figure 4 shows the RS spectral decomposition of a-C:H films synthesized at different DC discharge power. As can be seen from the figures, RS spectra are decomposed into three normal distribution bands designated as T, D and G. Frequency of the G peak varies in the range from 1550 to 1538 cm^{-1} and corresponds to a mode typical of C−C stretching with the symmetry E_{2g} (Figure 4).

The second peak designated as D is in the range of 1385−1365 cm^{-1} and represents a „breathing“ mode of hexagonal C_6 molecules with the symmetry A_{1g}. This mode is forbidden in ideal graphite and is enabled only when there is a certain number of degrees of freedom of C atoms in the hexagonal C_6 molecule. Appearance of vibrational degrees of freedom in C atoms causes structural deformation which in turn defines both disorder and certain order in the amorphous film grid. Thus, the occurrence of the D peak in the RS spectrum is associated with the presence of hexagonal C_6 molecules consisting of C atoms in the amorphous carbon film, which indicates the start of structural ordering. Occurrence of the T peak at 1260 cm^{-1} in the RS spectra of a-C:H films is caused by C−C stretching of the sp^3-sites [11,12].

It is important that the G mode in the frequency range from 1535 to 1550 cm^{-1} prevails in the Raman scattering spectra of most disordered carbon structures even when there is no order that is typical of graphite. Information on the sp^2/sp^3- bound C sites in a-C:H films may be taken from the G peak position. Comparison of the RS spectra of a-C:H films has shown that, as the power increases, center of the G peak shifts towards the low-frequency region: from 1550 to 1540 cm^{-1} in films synthesized on quartz substrates and from 1545 to 1538 cm^{-1} in films synthesized on silicon substrates. Shift of the center of Gpeak in amorphous carbon towards the low-frequency region is proportional to the increase in percentage of the sp^3-bound sites. Increase in the Tpeak intensity corresponding to the vibrational density of states (VDOS) of diamond-like clusters [11] and decrease in the D peak intensity are also observed. Changes of the T and D peak intensities as the DC discharge power increases indicate the increase in structural disorder and decrease in the volume fraction of carbon bonds with the sp^2- hybridization and diamond-like phase growth in the film structure [13].

Peak intensity ratio I_D/I_G is one of the key parameters characterizing the microstructure of disordered carbon structures. According to the Ferrari and Robertson three-step model [13], dependence between I_D/I_G and the content of sp^3-bound sites is nonlinear. It is known that, as I_D/I_G decreases, increase in the content of sp^3 increases and approaches zero when the content of sp^3 reaches approx. 50% in hydrogenated a-C:H films [11,14]. Therefore, consideration of the intensity ratio of T peaks caused by diamond clusters with sp^3-hybridization and the base G peak (I_T/I_G). Figure 5 shows the dependence of I_T/I_G on the discharge power. Increase in the DC discharge power leads to the growth of this ratio in a-C:H films, which indicates the increase in diamond-like structural units with the sp^3-bound sites.

Changes of the full width at half maximum (FWHM) of the G peak correlate with the changes of a-C:H films structure and properties [14]. FWHM(G) is one of the key variables characterizing the degree of disorder of a-C films structure. Structural disorder is induced by changes of valence angles and bond lengths in amorphous carbon. Low values of FWHM(G) are typical of amorphous carbon structures where the sp^2 clusters have less defects and are more ordered, while high values of FWHM(G) indicate the increasing disorder. According to Casiraghi's works [14,15],

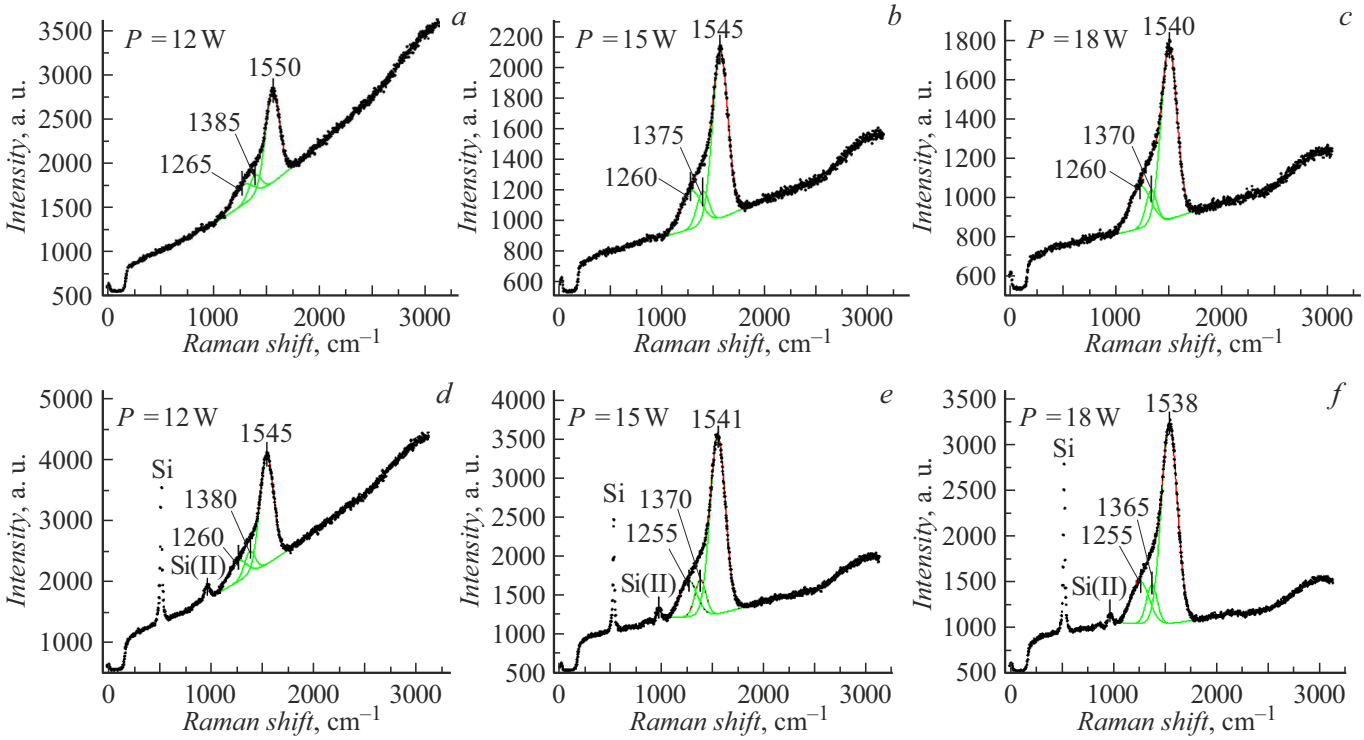

Figure 4. RS spectra decomposition of a-C:H films into the Gaussian components: *a*–*c* — films were prepared on a quartz substrate; *d*–*f* — films were prepared on silicon (100) substrates.

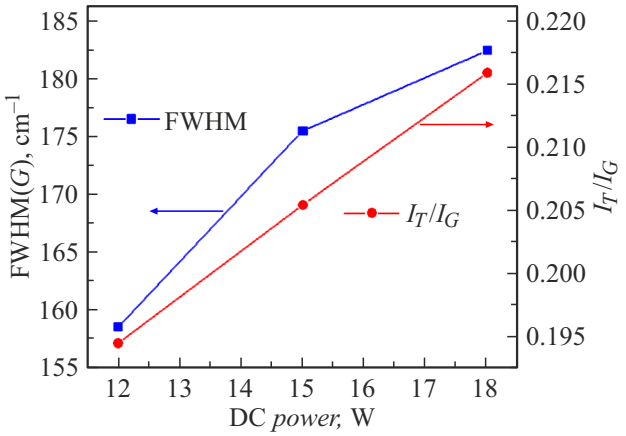

Figure 5. Dependence of the RS analysis variables of a-C:H films on the synthesis conditions.

increase in the content of sp^3- sites leads to the changes of bond lengths and also to the change of C–C bond valence angles. Figure 5 shows the change of FWHM(G) depending on discharge power. Increase in the discharge power leads to the FWHM(G) growth, which may be caused by considerable changes of angles and bond lengths in the a-C:H samples.

Figure 5 shows that FWHM(G) varies in the range from 158 to 182 cm^{-1}. Such changes of FWHM(G) may be assigned to amorphous disordered structures as shown in Ferrari's and Robertson's work [1]. With such values of FWHM(G) and an excitation energy of 2.6 eV, disorder in the structure consisting of sp^2-sites is smaller than 1 nm, i.e. full transition to the amorphous phase is observed.

2.3. Examination of the optical properties of a-C:H films depending on the ion-plasma discharge power

For optoelectronic instruments, optical properties of materials and controllability by varying synthesis conditions are critical. Structural modification of a-C:H films was carried out by varying synthesis conditions to influence the atomic structure formation considerably. Change of the number of sp^2- and sp^3- sites and, consequently, relation of the sites have considerable influence on the electronic properties of films. Type of hybridization defines the features of formation of energy bands in amorphous carbon films, which in turn leads to the differences in optical properties. Optical characteristics such as absorption, transparency and refraction depend on sp^2/sp^3 and may be adapted by varying synthesis conditions to offer new possibilities for the development of high-performance optoelectronic materials.

Figure 6 shows the changes of refractive index of a-C:H films synthesized on quartz substrates depending on the DC discharge power. Refractive index of a-C:H films may vary in a wide range depending on the content of sp^2- and sp^3- sites of carbon bonds in the film structure [4]. Figure 6 shows that the refractive index of synthesized a-C:H films

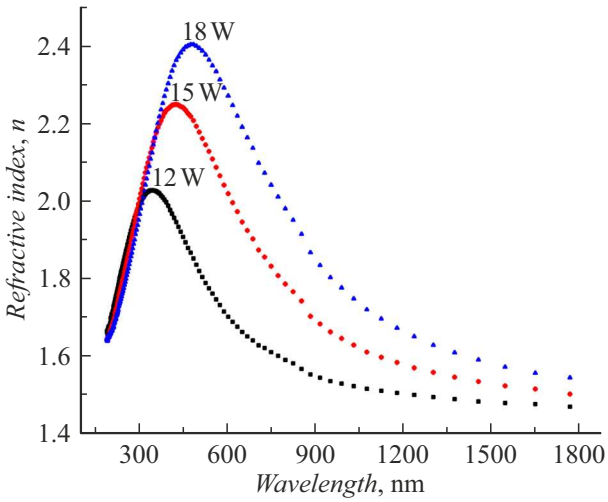

Figure 6. Spectral dependence of the refraction index of a-C:H films synthesized at different DC discharge powers.

increases for all samples as the discharge power grows. The maximum refractive index (with fixed wavelength 589 nm, $n = 2.29$) corresponds to a film made at a discharge power of 18 W. Moreover, a significant shift towards the long-wavelength region of the refractive index peak maximum of a-C:H films at various excitation wavelengths in the range from 345 to 487 nm. Increase in the refractive index and shift of its maximum with the increase in power may be associated with the change of film structure, i.e. change of sp^2- and sp^3- carbon configuration bonds.

The refractive index defines the degree to which the incident radiation changes its direction when it is transmitted through the medium. In film structures, an increase in the fraction of sp^2-hybridized sites gives rise to pentahedral, hexahedral or heptahedral molecules and chains. sp^3-hybridization often gives rise to more closely-packed three-dimensional tetrahedral structures. RS results show that the increase in the content of sp^3-bound sites gives rise to clusters that are different in order and size, distortion of hexagonal rings with sp^2-bonds, increase in defects and decrease in the number of ordered rings. In films with many three-dimensional structural units and ring structure defects, light may interact with them in a large volume by changing the propagation direction, which causes higher refractive indices. Thus, the fraction of sp^3-hybridized carbon atoms films deposited at higher power with higher refractive indices is higher than that in samples made at lower discharge powers.

Optical transmittance spectra (T) of the synthesized samples were studied in the wavelength range from 190 nm to 1100 nm. Changes of optical transmittance spectra of a-C:H films are shown in Figure 7, *a*. As shown in figure, film transparency decreases considerably as the DC discharge power increases, in particular for samples synthesized at a discharge power of 18 W. As mentioned above, a-C:H films are characterized by a disordered structure. This disorder and the presence of defects may change the atom and electron density o a material. The induced defects may form local energy levels in the band gap or excited states that serve as additional light absorption channels. The decrease in transparency may be caused by the increase in light absorption on the additionally formed density of allowed states or with more intense light scattering on defects in the synthesized samples. These processes may reduce considerably the efficiency of light transmission through samples. Also note that all films have transmission coefficients of $T > 90\%$ in a large wavelength range (≥ 800 nm), which is indicative of their transparency in the near IR range.

Optical band gap of amorphous carbon films is a structurally sensitive parameter and may vary in a wide range depending on synthesis conditions. This study used spectral dependences of the absorption coefficient in the studied wavelength range to calculate the band gap by Tauc's method [16] that is applicable to semiconductor materials. E_g was defined in the region of $\alpha \sim 10^5\,\mathrm{cm}^{-1}$ and provided that $\alpha \cdot d \sim 1$, where d is the film thickness that varies in the range from 45 nm to 70 nm. Change of the band gap of synthesized films depending on the discharge power is shown in Figure 7, *b*. As can be seen from the figure, the band gap E_g of synthesized samples varies from 1.8 eV to 1.43 eV. It was found that the band gap decreases in the a-C:H samples as the discharge power increases.

Decrease in the band gap in synthesized films with the increase in power is accompanied by growth of their structural disorder due to different configurations of C−C- and C−H bonds with sp^3-hybridization. Optical band gap of a-C:H films depends on sp^2/sp^3- bonds. Hydrogen introduction facilitates the passivation of free π-electrons in the sp^2 sites, thus, increasing the fraction of the sp^3-hybridized (C−C and C−H) bonds. Formed tetrahedral bonds enhance the structural disorder in films. Moreover, the increase in energy of condensed atoms causes not only and not so much the change of short-range order as the change of medium-range structural order in the amorphous film. According to [17,18], the medium-range structural order plays a significant role in formation of edges and affects the band gap width.

According to the cluster model, the electronic structure of a-C:H films is formed from π- and π^* states inside the σ- and σ^*-bands. π- and π^*-states form valence band and conduction band edges inducing additional localized states, which affects the change of the amorphous carbon band gap width. The presence of hydrogen has a slight impact on formation of band structure because the states formed by σ-bonds in the C−H compound are energetically farther from the band gap edge [17,19].

Increase in the sp^3-clusters with σ-bonds that form the a-C:H matrix causes the change in distribution of the tails of localized states within the band gap. This in turn changes the length of tails and density of localized states on band edges. Examination of the band gap width shows that E_g

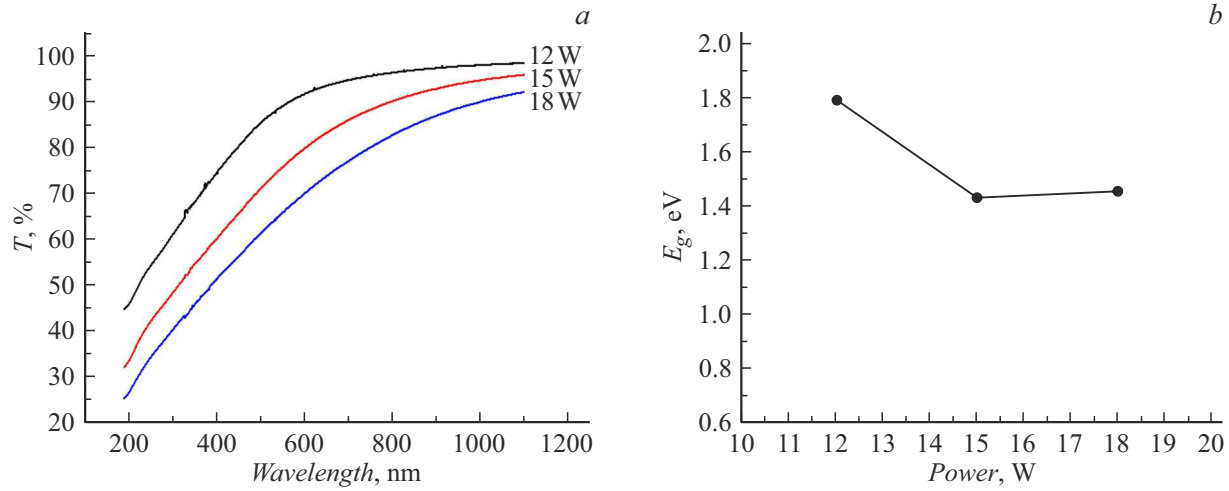

Figure 7. Optical transmittance spectra (a) and band gap (b) in a-C:H films depending on the DC discharge power.

may be controlled not only by the state of π-electrons, but also by the degree of structural disorder of a-C:H films.

According to Robertson's work [20], the maximum density and hardness of a-C:H films are reached at a band gap width of 1.4 eV, and such films are classified as most „diamond-like“ structures with the desired content of sp^3-sites.

Conclusion

The magnetron ion-plasma sputtering method was used to make amorphous hydrogenated carbon films passivated by H atoms at different discharge powers. The studies have shown that the structure and optical properties of a-C:H films may be controlled by varying the synthesis conditions. It was found from the RS spectra that the increase in DC discharge power facilitates the growth of sp^2/sp^3-hybridized bonds, which in turn affects the formation of local film structure.

Changes of optical properties correlate with structural changes. Studies of optical properties have shown that the refractive index of the deposited a-C:H films varies from 1.71 to 2.29 (at 589 nm) and depends on the deposition conditions. Synthesis at high DC discharge power provides films with higher refractive index. Moreover, the synthesized a-C:H films have the transmission coefficient $T > 90\%$ in the near IR region which makes them a promising material for utilization as protective and antireflection coatings for infrared optics. Increase in the DC discharge power causes the change of band gap from 1.8 eV to 1.43 eV. This significant change of the optical band gap makes it possible to use a-C:H films for creating new optical instruments and devices based on photon calculations.

Funding

The study was supported by grant № AP19676270 provided by the Ministry of Science and Higher Education of the Republic of Kazakhstan.

Conflict of interest

The authors declare no conflict of interest.

References

[1] A.C. Ferrari, J. Robertson. Philosophical Transactions Royal Society of London. Series A: Math., Phys. Eng. Sci., **362** (1824), 2477 (2004). DOI: 10.1098/rsta.2004.1452
[2] W.E.S.S. Viana, A.E. Elzubair, M.M. Wysard, D.F. Franceschini, S.S. Camargo. Thin Solid Films, **695**, 137733 (2020). DOI: 10.1016/j.tsf.2019.137733
[3] I.S. Kim, Ch.-E. Shim, S.W. Kim, Ch.-S. Lee, J. Kwon, K.-E. Byun, U. Jeong. Adv. Mater., **35** (43), 2204912 (2023). DOI: 10.1002/adma.202204912
[4] J. Li, H. Chae. Korean J. Chem. Eng., **40** (6), 1268 (2023). DOI: 10.1007/s11814-023-1443-x
[5] S. Karmakar, M.A. Halim, M. Sultana, P.K. Sarkar, I.H. Emu, A.M. Jaimes-Leal, A. Haque. Diamond Related Mater., **146**, 111196 (2024). DOI: 10.1016/j.diamond.2024.111196
[6] M. Steinhorst, M. Giorgio, T. Roch, Ch. Leyens. ACS Appl. Mater. Interfaces, **15** (44), 51704 (2023). DOI: 10.1021/acsami.3c10719
[7] A.P. Ryaguzov, R.R. Nemkayeva, O.I. Yukhnovets, N.R. Guseinov, S.L. Mikhailova, F. Bekmurat, A.R. Assembayeva. Opt. Spectr., **127**, 251 (2019). DOI: 10.1134/S0030400X19080228
[8] A.P. Ryaguzov, B.E. Alpysbayeva, R.R. Nemkayeva, R.K. Aliaskarov, O.I. Yukhnovets, D.M. Mamyrbayeva. Eurasian Phys. Tech. J., **12**, 2(24), 48 (2015).
[9] J. Robertson. Diamond Related Mater., **4** (4), 297 (1995). DOI: 10.1016/0925-9635(94)05264-6
[10] J. Robertson. Diamond Related Mater., **3** (4–6), 361 (1994). DOI: 10.1016/0925-9635(94)90186-4

[11] A.C. Ferrari, J. Robertson. Phys. Rev. B, **61**, 14095 (2000). DOI: 10.1103/PhysRevB.61.14095
[12] A.P. Ryaguzov, G.A. Yermekov, T.E. Nurmamytov, R.R. Nemkayeva, N.R. Guseinovet, R.K. Aliaskarov. J. Mater. Res., **31**, 127 (2016). DOI: 10.1557/jmr.2015.391
[13] A.C. Ferrari. Diamond Related Mater., **11** (3–6), 1053 (2002). DOI: 10.1016/S0925-9635(01)00730-0
[14] C. Casiraghi, A.C. Ferrari, J. Robertson. Phys. Rev. B, **72** (8), 085401 (2005). DOI: 10.1103/PhysRevB.72.085401
[15] C. Casiraghi, F. Piazza, A.C. Ferrari, D. Grambole, J. Robertson. Diamond Related Mater., **14** (3-7), 1098 (2005). DOI: 10.1016/j.diamond.2004.10.030
[16] J. Tauc. Progr. Semiconductors, **9**, 87 (1965). DOI: 10.3367/UFNr.0094.196803e.0501
[17] J. Robertson, E.P. O'Reilly. Phys. Rev. B, **35** (6), 2946 (1987). DOI: 10.1103/physrevb.35.2946
[18] Sh.Sh. Sarsembinov, O.Yu. Prikhodko, A.P. Ryaguzov, S.Ya. Semicond. Sci. Technol., **16**, 872 (2001). DOI: 10.1088/0268-1242/16/10/310
[19] M. Chhowalla, J. Robertson, C.W. Chen, S.R.P. Silva, C.A. Davis, G.A.J. Amaratunga, W.I. Milne. J. Appl. Phys., **81** (1), 139 (1997). DOI: 10.1063/1.364000
[20] J. Robertson. Mat. Sci. Eng. R, **37** (4–6), 129 (2002). DOI: 10.1016/S0927-796X(02)00005-0

Translated by E.Ilinskaya